Journal of the Serbian Society for Computational Mechanics / Vol. 3 / No. 2, 2009 / pp. 56-66

(UDC: 539.3:519.876.5)

Computational Simulation of Continua with Isotropic Surface Potentials

A. Javili[1], P. Steinmann[1]

[1]Chair of Applied Mechanics
University of Erlangen-Nuremberg, Egerlandstraße 5, D-91058 Erlangen
e-mail: ali.javili@ltm.uni-erlangen.de, paul.steinmann@ltm.uni-erlangen.de

Abstract

Common modeling in continuum mechanics takes exclusively the bulk into account, nevertheless, neglecting possible contributions from the boundary. However, surface effects sometimes play a dominant role in the material behavior, the most prominent example being surface tension. Within this contribution surface potentials at the boundary are allowed, in general, to depend not only on the boundary deformation but also on the boundary deformation gradient. Motivated by this idea, a suitable finite element framework based on rank deficient deformation gradients is established. In essence, the total potential energy functional that we seek to minimize with respect to all admissible spatial variations at fixed material placement is consisting of both contributions from the bulk and the boundary.

Keywords: Surface potentials, Surface tension

1. Introduction

Surfaces of bodies and interfaces between pairs of bodies, in general, exhibit properties different from those associated with the bulk. This fact has been studied in the literature since the milestone work by (Gibbs, 1906) and elaborated by others, e.g. (Adam, 1941; Gurtin, 1974; Gurtin and Murdoch, 1975; Leo and Sekerka, 1989; Adamson and Gast, 1997; Simha and Bhattacharya, 2000; Steinmann and Häsner, 2005; Fischer et al., 2008). Moreover, in material processing, the boundary of material is frequently exposed to e.g., oxidation, ageing, grit blasting, plasma jet treatment, etc., thus obviously resulting in distinctively different properties in comparatively thin boundary layers. Likewise coating materials with thin films results clearly in different properties at the boundary. These effects could phenomenologically be modelled in terms of boundaries equipped with their own potential energy.

The numerical simulation of the surface of the body has been studied extensively when the bulk behaves like a fluid, e.g. (Navti et al., 1997; Bellet, 2001; Dettmer at al., 2003; Dettmer and Peri c′, 2006) and also, based on a variational formulation in (Olson and Kock, 1994; Saksono and Peri c′, 2006a; Saksono and Peri c′, 2006b). In (Steinmann, 2008) a systematic treatment of the boundary surface and its coupling with the bulk based on potentials was proposed. In this respect different behaviors for the surface of the continuum body can be considered by defining the respective surface potential energy. In this contribution the computational implementation of such boundary potentials is studied and in order to determine

the behavior of the surface and the efficiency of the numerical framework, different boundary material models, together with their corresponding numerical examples, are proposed.

2. Theory and FE-Formulation

To introduce our notations we briefly outline the basic equations of the geometry of boundaries, i.e. surfaces in 3D. Furthermore, the weak form and the discretized form of the balance equations are formulated in this section.

2.1 Geometry and kinematics of boundaries

A two-dimensional (smooth) surface $\mathcal{S}$ in the three-dimensional, embedding Euclidean space with coordinates $\boldsymbol{x}$ is parameterized by two surface coordinates ξ^α with $\alpha = 1, 2$. Therefore,

$$\boldsymbol{x} = \boldsymbol{x}\left(\xi^\alpha\right). \tag{1}$$

The corresponding tangent vectors $\boldsymbol{a}_\alpha \in T\mathcal{S}$ to the surface coordinate lines ξ^α, i.e. the covariant (natural) surface basis vectors are given by

$$\boldsymbol{a}_\alpha = \partial_{\xi^\alpha} \boldsymbol{x}. \tag{2}$$

The associated contravariant (dual) surface basis vectors $\boldsymbol{a}^\alpha$ can be defined by the Kronecker property $\delta^\alpha_\beta = \boldsymbol{a}^\alpha \cdot \boldsymbol{a}_\beta$. More details on the geometry of the surfaces can be found in (Ciarlet, 2006) and (Steinmann, 2008). The contra- and covariant base vectors $\boldsymbol{a}^3$ and $\boldsymbol{a}_3$, normal to $T\mathcal{S}$, are defined respectively so that $\boldsymbol{a}^3 \cdot \boldsymbol{a}_3 = 1$. Accordingly, the surface normal $\boldsymbol{n}$ is computed as

$$\boldsymbol{n} = \boldsymbol{a}_1 \times \boldsymbol{a}_2 / |\, \boldsymbol{a}_1 \times \boldsymbol{a}_2 \,|. \tag{3}$$

Moreover, the mixed-variant surface unit tensor $\hat{\boldsymbol{i}}$ is defined as

$$\hat{\boldsymbol{i}} := \boldsymbol{a}_\alpha \otimes \boldsymbol{a}^\alpha = \boldsymbol{i} - \boldsymbol{n} \otimes \boldsymbol{n}, \tag{4}$$

in which $\boldsymbol{i}$ represents the ordinary mixed-variant unit tensor of the three-dimensional embedding Euclidean space. Finally, the surface gradient and surface divergence operators for vector fields are defined by:

$$\widehat{\operatorname{grad}}\{\bullet\} := \partial_{\xi^\alpha}\{\bullet\} \otimes \boldsymbol{a}^\alpha \quad \text{and} \quad \widehat{\operatorname{div}}\{\bullet\} := \partial_{\xi^\alpha}\{\bullet\} \cdot \boldsymbol{a}^\alpha. \tag{5}$$

Consider next a continuum body that takes the material configuration $\mathcal{B}_0$ at time $t = 0$ with the surface $\mathcal{S}_0$ attached to the body and respectively, takes the spatial configuration $\mathcal{B}_t$ at time $t > 0$ with the surface $\mathcal{S}_t$. The placement $\boldsymbol{x}$ and $\boldsymbol{X}$ in the spatial and the material configurations are related by the invertible (nonlinear) deformation map

$$\boldsymbol{x} = \boldsymbol{\varphi}\left(\boldsymbol{X}\right). \tag{6}$$

The associated deformation gradient or rather (invertible) linear tangent map between material and spatial line elements $\mathrm{d}\boldsymbol{x} \in T\mathcal{B}_t$ and $\mathrm{d}\boldsymbol{X} \in T\mathcal{B}_0$ is defined as

$$\boldsymbol{F} := \text{Grad}\ \boldsymbol{\varphi}(\boldsymbol{X}) \qquad \text{with Jacobian } J := \frac{\mathrm{d}v}{\mathrm{d}V} = \det \boldsymbol{F} > 0. \tag{7}$$

The surface deformation gradient $\widehat{\boldsymbol{F}}$ or rather (non-invertible) linear surface tangent map between line elements $\mathrm{d}\boldsymbol{X} \in T\mathcal{S}_0$ and $\mathrm{d}\boldsymbol{x} \in T\mathcal{S}_t$ is defined as

$$\widehat{\boldsymbol{F}} := \widehat{\text{Grad}}\ \boldsymbol{\varphi}(\boldsymbol{X}) = \boldsymbol{a}_\alpha \otimes \boldsymbol{A}^\alpha. \tag{6}$$

2.2 Dirichlet principle of minimum potential energy

The bulk potential energy density U_0 per material unit volume in $\mathcal{B}_0$ is composed of internal and external contributions W_0 and V_0, respectively, as

$$U_0 = W_0 + V_0 \quad \text{with} \quad W_0 = W_0(\boldsymbol{F}; \boldsymbol{X}) \qquad \text{and} \qquad V_0 = V_0(\boldsymbol{\varphi}; \boldsymbol{X}). \tag{8}$$

Likewise, the surface potential energy density u_0 per material unit length in $\mathcal{S}_0$ may consist of internal and external contributions w_0 and v_0, respectively, as

$$u_0 = w_0 + v_0 \quad \text{with} \quad w_0 = w_0(\widehat{\boldsymbol{F}}; \boldsymbol{X}) \qquad \text{and} \qquad v_0 = v_0(\boldsymbol{\varphi}; \boldsymbol{X}). \tag{9}$$

In summary, the total potential energy functional $I = I(\boldsymbol{\varphi})$ that we seek to minimize with respect to all admissible variations $\delta\boldsymbol{\varphi}$ (spatial variations at fixed material placement) reads

$$I(\boldsymbol{\varphi}) := \int_{\mathcal{B}_0} U_0(\boldsymbol{\varphi}, \boldsymbol{F}; \boldsymbol{X})\ \mathrm{d}V + \int_{\mathcal{S}_0} u_0(\boldsymbol{\varphi}, \widehat{\boldsymbol{F}}; \boldsymbol{X})\ \mathrm{d}A. \tag{10}$$

Then the minimization of the total potential energy functional, $\delta I(\boldsymbol{\varphi}) = 0$, renders the weak form of the (local) balance equations including contributions from the boundary terms

$$\begin{aligned} \int_{\mathcal{B}_0} \boldsymbol{P} : \text{Grad}\,\delta\boldsymbol{\varphi}\ \mathrm{d}V \ &+ \int_{\mathcal{S}_0} \widehat{\boldsymbol{P}} : \widehat{\text{Grad}}\,\delta\boldsymbol{\varphi}\ \mathrm{d}A \\ &= \int_{\mathcal{B}_0} \boldsymbol{b}_0 \cdot \delta\boldsymbol{\varphi}\ \mathrm{d}V + \int_{\mathcal{S}_0} \hat{\boldsymbol{b}}_0 \cdot \delta\boldsymbol{\varphi}\ \mathrm{d}A \qquad \forall \delta\boldsymbol{\varphi}. \end{aligned} \tag{11}$$

The stress in two-point description and the distributed (volume) force related to the bulk $\mathcal{B}_0$ are defined, as usual, as

$$\boldsymbol{P} := \partial_{\boldsymbol{F}} U_0 \qquad \text{and} \qquad \boldsymbol{b}_0 := -\partial_{\boldsymbol{\varphi}} U_0. \tag{12}$$

Likewise, the stress in two-point description and the distributed force (the surface load or rather tractions) related to the surfaces in $\mathcal{S}_0$ are defined as

$$\widehat{\boldsymbol{P}} := \partial_{\widehat{\boldsymbol{F}}} u_0 \qquad \text{and} \qquad \hat{\boldsymbol{b}}_0 := -\partial_{\boldsymbol{\varphi}} u_0. \tag{13}$$

Moreover, by applying the divergence theorem in the bulk and at the boundary, after some manipulations, equation (11) is cast into

$$-\int_{\mathcal{B}_0} \delta\boldsymbol{\varphi}\cdot\mathrm{Div}\,\boldsymbol{P}\ \mathrm{d}V - \int_{\mathcal{B}_0} \delta\boldsymbol{\varphi}\cdot\boldsymbol{b}_0\ \mathrm{d}V + \int_{\mathcal{S}_0} \delta\boldsymbol{\varphi}\cdot\boldsymbol{P}\cdot\boldsymbol{N}\ \mathrm{d}A$$
$$- \int_{\mathcal{S}_0} \delta\boldsymbol{\varphi}\cdot\widehat{\mathrm{Div}}\,\widehat{\boldsymbol{P}}\ \mathrm{d}A - \int_{\mathcal{S}_0} \delta\boldsymbol{\varphi}\cdot\hat{\boldsymbol{b}}_0\ \mathrm{d}A = 0 \quad \forall\delta\boldsymbol{\varphi}. \tag{14}$$

Since the above expression holds for all spatial variations, it renders the equivalent local expressions, i.e. the (localized) force balance in the bulk $\mathcal{B}_0$ and the (localized) force balance or Neumann-type boundary condition on the boundary surfaces in $\mathcal{S}_0 = \partial\mathcal{B}_0$. More details on this is given in (Steinmann, 2008).

2.3 Finite element formulation

In order to have an efficient finite element framework, the surface elements are chosen to be consistent with the bulk. For instance, if the bulk is discretized by means of quadratic tetrahedra, the surface elements are quadratic triangles.

The principle of virtual work achieved in (14) is discretized into a set of bulk elements and a set of surface elements with

$$\mathcal{B}_0 = \bigcup_{\beta=1}^{n_{b-el}} \mathcal{B}_0^{\beta} \qquad \mathcal{S}_0 = \bigcup_{\gamma=1}^{n_{s-el}} \mathcal{S}_0^{\gamma}, \tag{15}$$

where n_{b-el} stands for the number of bulk elements and n_{s-el} stands for the number of surface elements. In the current manuscript the discretization procedure for the bulk is skipped, for the sake of space. Nevertheless, a similar strategy can be used as has been introduced in the literature, e.g., (Zienkiewicz and Taylor, 2005).

The geometry for each surface element can be written as a function of natural coordinate $\boldsymbol{\xi}$ by using standard interpolations and Galerkin approximations.

$$\boldsymbol{\varphi}(\boldsymbol{\xi}) \approx \sum_{i=1}^{N_{node}} \widehat{N}^i(\boldsymbol{\xi})\boldsymbol{\varphi}^i \qquad \text{and} \qquad \boldsymbol{X}(\boldsymbol{\xi}) \approx \sum_{i=1}^{N_{node}} \widehat{N}^i(\boldsymbol{\xi})\boldsymbol{X}^i. \tag{16}$$

Here $\boldsymbol{\xi} = (\xi_1, \xi_2)$ are the natural coordinates in two dimensions and $\widehat{N}^i$ is the standard shape function of the surface element at node i. Furthermore, the surface deformation gradient results in

$$\widehat{\boldsymbol{F}} = \widehat{\mathrm{Grad}}\boldsymbol{\varphi} \approx \sum_{i=1}^{N_{node}} \boldsymbol{\varphi}^i \otimes \widehat{\mathrm{Grad}}\,\widehat{N}^i. \tag{17}$$

Equipped with all the above formulae, the weak form of the balance equation associated with bulk element β with attached surface elements γ for the node i is eventually discretized into

$$\int_{\mathcal{B}_0^{\beta}} \boldsymbol{P}\cdot\mathrm{Grad}\,N^i\ \mathrm{d}V + \int_{\mathcal{S}_0^{\gamma}} \widehat{\boldsymbol{P}}\cdot\widehat{\mathrm{Grad}}\,\widehat{N}^i\ \mathrm{d}A = \int_{\mathcal{B}_0^{\beta}} \boldsymbol{b}_0 N^i\ \mathrm{d}V + \int_{\mathcal{S}_0^{\gamma}} \hat{\boldsymbol{b}}_0\widehat{N}^i\ \mathrm{d}A. \tag{18}$$

In order to solve (18), the Newton-Raphson scheme can be employed. For that, first the residual vector for each local node i associated with the bulk element β with attached surface elements γ, is defined as

$$\boldsymbol{R}_e^i = \int_{\mathcal{B}_0^\beta} \boldsymbol{P} \cdot \mathrm{Grad}\, N^i \; \mathrm{d}V + \int_{\mathcal{S}_0^\gamma} \widehat{\boldsymbol{P}} \cdot \widehat{\mathrm{Grad}}\, \widehat{N}^i \; \mathrm{d}A - \int_{\mathcal{B}_0^\beta} \boldsymbol{b}_0 N^i \; \mathrm{d}V - \int_{\mathcal{S}_0^\gamma} \hat{\boldsymbol{b}}_0 \widehat{N}^i \; \mathrm{d}A. \tag{19}$$

The global residual at the global node J is defined by

$$\boldsymbol{R}^J := \mathop{\mathsf{A}}_{e=1}^{n_{el}} \boldsymbol{R}_e^j \tag{20}$$

where the corresponding local node number in an element or surface element e to the global node number J is denoted by $j = 1, n_{ne}$ and n_{ne} is the number of nodes per element or surface element. Herein the operator $\mathop{\mathsf{A}}_{e=1}^{n_{el}}$ denotes the assembly of all element and surface elements contributions at the global node $J = 1, n_{np}$ where n_{np} is the total number of nodes.

The consistent linearization of of the resulting system of equations, would be

$$\boldsymbol{R}(\boldsymbol{d}) + \frac{\partial \boldsymbol{R}}{\partial \boldsymbol{d}}\bigg|_n \Delta \boldsymbol{d} = \boldsymbol{0} \qquad \text{and} \qquad \boldsymbol{d}_{n+1} = \boldsymbol{d}_n + \Delta \boldsymbol{d}, \tag{21}$$

in which n stands for the iteration step and $\boldsymbol{R}$ and $\boldsymbol{d}$ are the global vectors of residual and spatial coordinates. Solving (21) results in the spatial coordinate increment, $\Delta \boldsymbol{d}$ and consequently $\boldsymbol{d}_{n+1}$.

The local tangent stiffness would be

$$\begin{aligned} \left[\boldsymbol{K}_e^{ij}\right]_{ac} = \left[\frac{\partial \boldsymbol{R}_e^i}{\partial \boldsymbol{\varphi}^j}\right]_{ac} &= \int_{\mathcal{B}_0^\beta} \left\{\mathrm{Grad}\, N^i\right\}_b \left\{\mathbb{A}\right\}_{abcd} \left\{\mathrm{Grad}\, N^j\right\}_d \; \mathrm{d}V \\ &+ \int_{\mathcal{S}_0^\gamma} \left\{\widehat{\mathrm{Grad}}\, \widehat{N}^i\right\}_b \left\{\widehat{\mathbb{A}}\right\}_{abcd} \left\{\widehat{\mathrm{Grad}}\, \widehat{N}^j\right\}_d \; \mathrm{d}A, \end{aligned} \tag{22}$$

in which $\mathbb{A}$ is the fourth-order elasticity two-point tensor as has been introduced in (Marsden and Hughes, 1994). $\widehat{\mathbb{A}}$ is defined, in analogy, as follows:

$$\mathbb{A} = \frac{\partial \boldsymbol{P}}{\partial \boldsymbol{F}} \qquad \text{and} \qquad \widehat{\mathbb{A}} = \frac{\partial \widehat{\boldsymbol{P}}}{\partial \widehat{\boldsymbol{F}}}. \tag{23}$$

Finally in analogy to (20), the global tangent stiffness of the whole system has to be assembled

$$\boldsymbol{K}^{IJ} = \mathop{\mathsf{A}}_{e=1}^{n_{el}} \boldsymbol{K}_e^{ij}. \tag{24}$$

It is noteworthy that the assembly operator introduced here is slightly different from that introduced in the literature, e.g. (Zienkiewicz and Taylor, 2005), in the sense that here the contributions from both the bulk and the boundary surface have to be taken into account.

3. Examples of surface potentials

In order to model a specific material behavior of the boundary, first the internal potential energy of the boundary material, $w_0(\widehat{\boldsymbol{F}}; \boldsymbol{X})$, is defined. Next, the corresponding derivations are carried

out so as to achieve the boundary Piola stress and elasticity tensor $\hat{\boldsymbol{P}}$ and $\hat{\mathbb{A}}$, respectively. In this contribution two elementary options are proposed for isotropic surface potentials in sections § 3.1 and § 3.2, respectively. The first option models boundaries which behave like a neo-Hookean material and the second one models the typical surface tension.

3.1 Neo-Hookean type boundary potential

For a boundary material which behaves analogously to a neo-Hookean material, however in two dimensions, so that it mimics the format e.g. advocated in (Kuhl et al., 2004), the internal potential energy can be expressed as

$$w_0(\widehat{\boldsymbol{F}}) = \frac{1}{2}\hat{\lambda}\log^2\hat{J} + \frac{1}{2}\hat{\mu}[\widehat{\boldsymbol{F}} : \widehat{\boldsymbol{F}} - 2 - 2\log\hat{J}]. \tag{25}$$

The corresponding boundary Piola stress tensor takes the following explicit expression

$$\hat{\boldsymbol{P}} = \frac{\partial w_0}{\partial \widehat{\boldsymbol{F}}} = \hat{\lambda}\log\hat{J}\widehat{\boldsymbol{F}}^{-T} + \hat{\mu}\left[\widehat{\boldsymbol{F}} - \widehat{\boldsymbol{F}}^{-T}\right]. \tag{26}$$

Moreover, the explicit representations for the fourth order elasticity tensor $\hat{\mathbb{A}}$ will be

$$\hat{\mathbb{A}} = \frac{\partial \hat{\boldsymbol{P}}}{\partial \widehat{\boldsymbol{F}}} = \hat{\lambda}\,\widehat{\boldsymbol{F}}^{-T} \otimes \widehat{\boldsymbol{F}}^{-T} + \hat{\mu}\,\hat{\mathbb{I}} + \left[\hat{\lambda}\log\hat{J} - \hat{\mu}\right]\hat{\mathbb{D}}, \tag{27}$$

in which

$$\hat{\mathbb{I}} = \frac{\partial \widehat{\boldsymbol{F}}}{\partial \widehat{\boldsymbol{F}}} = \boldsymbol{I}\overline{\otimes}\hat{\boldsymbol{I}} \quad \text{with} \quad \left\{\boldsymbol{A}\overline{\otimes}\boldsymbol{B}\right\}_{ijkl} = A_{ik}\,B_{jl} \quad \text{and} \quad \hat{\mathbb{D}} = \frac{\partial \widehat{\boldsymbol{F}}^{-T}}{\partial \widehat{\boldsymbol{F}}}. \tag{28}$$

3.1.1 Numerical example

In order to illustrate the effect of the neo-Hookean type surface potential, a model as shown in the Figure 1 resembling the Cook's membrane, however in three dimensions, is considered.

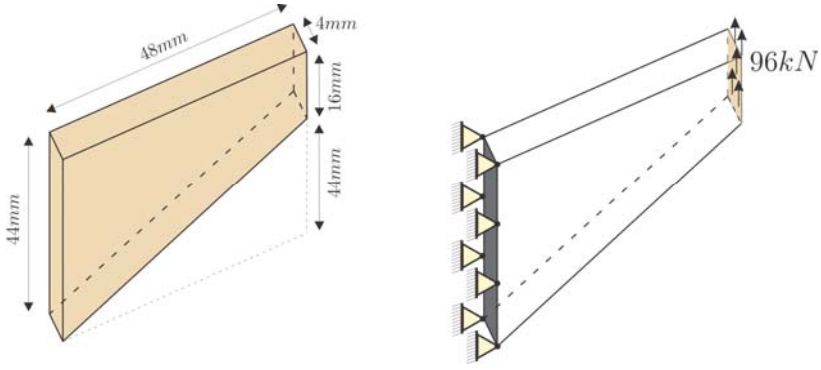

Figure 1. A model to illustrate the surface potential effects

The structure is fixed in all the degrees of freedom on the left wall and a distributed force of $0.75\,kN/mm^2$ is applied on the right wall in the upward direction as depicted in the Figure.

The material parameters for the bulk are $\mu = 8\ GPa$ and $\lambda = 12\ GPa$. On the lateral walls of the structure the neo-Hookean boundary potential is applied with the surface material parameters $\hat{\mu}$ and $\hat{\lambda} = 1.5\hat{\mu}$. The results are shown in the Figure 2 for different ratios of $\hat{\mu}/\mu = \hat{\lambda}/\lambda = 0, 0.1, 1, 10m$. The increase of the energy contribution from the boundary results in more stiffness of the material and thus, for the same applied load, less displacement.

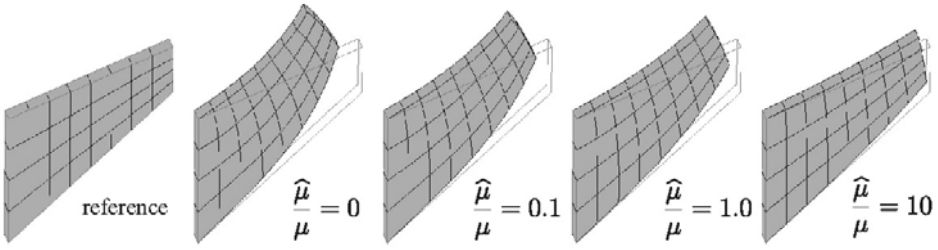

Figure 2. Illustration of the neo-Hookean type surface resistance

3.2 Surface tension boundary potential

The second material model for the boundary captures the surface effects in fluids, i.e. surface tension; more details can be found in (Lifshitz and Landau, 1987). For this model the potential energy per unit deformed area has to be constant due to constant surface tension on the whole boundary, see e.g. (Gurtin, 1975). Therefore

$$w_t = \text{const.} = \hat{\gamma} \tag{29}$$

and correspondingly

$$w_0(\widehat{\boldsymbol{F}}) = \hat{\gamma}\hat{J}. \tag{30}$$

The associated boundary Piola stress tensor takes the following explicit expression

$$\widehat{\boldsymbol{P}} = \frac{\partial w_0}{\partial \widehat{\boldsymbol{F}}} = \hat{\gamma}\hat{J}\,\widehat{\boldsymbol{F}}^{-T}. \tag{31}$$

Moreover, the explicit representations for the fourth order elasticity tensor $\hat{\mathbb{A}}$ will be

$$\hat{\mathbb{A}} = \frac{\partial \widehat{\boldsymbol{P}}}{\partial \widehat{\boldsymbol{F}}} = \hat{\gamma}\hat{J}[\widehat{\boldsymbol{F}}^{-T} \otimes \widehat{\boldsymbol{F}}^{-T} + \hat{\mathbb{D}}]. \tag{32}$$

Remark. For the surface tension model one has to notice that the energy of the surface, in general, will not be minimum in the reference configuration which may lead to computational instabilities, see (Javili and Steinmann, 2009) for more details.

3.2.1 Numerical example

As an example, due to the surface tension effect, the surface of a body tends to obtain constant mean curvature, i.e. a cube tends to transform to a sphere. In order to illustrate this fact, a cube as shown in Figure 3 (top-left corner) is considered which is fixed in the center in the translational as well as the rotational degrees of freedom. For the bulk the neo-Hookean

material model is assumed. By increasing the material parameters $\hat{\gamma}$ the cube gradually transforms to a sphere.

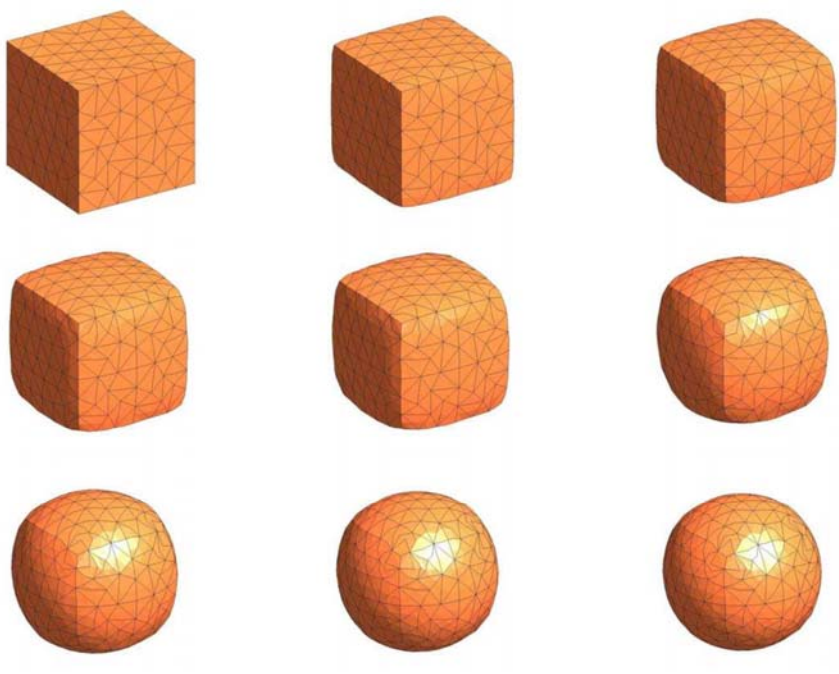

Figure 3. Transformation of a cube to sphere due to surface tension

3.2.2 Numerical example

This example is carried out in order to investigate deeper the isotropic surface tension effects and also to study the efficiency of the finite elements. The model is a hollow cylinder with the dimensions shown in the Figure 4 and fixed at both ends. The surface tension boundary potentials are assigned to the model. By increasing the surface tension, $\hat{\gamma}$, the model resembles the well-known liquid bridge (or soap film) example.

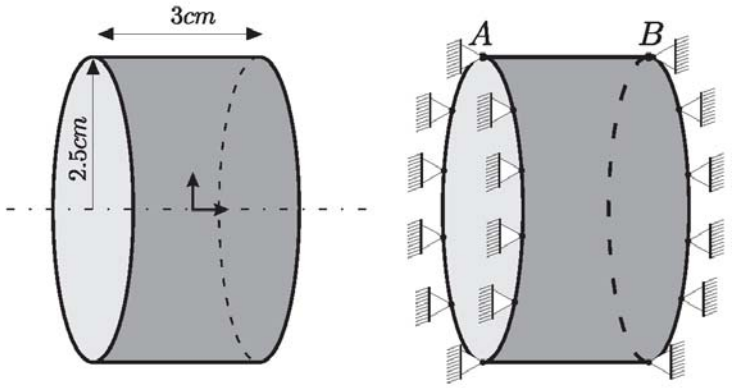

Figure 4. A model (hollow) cylinder

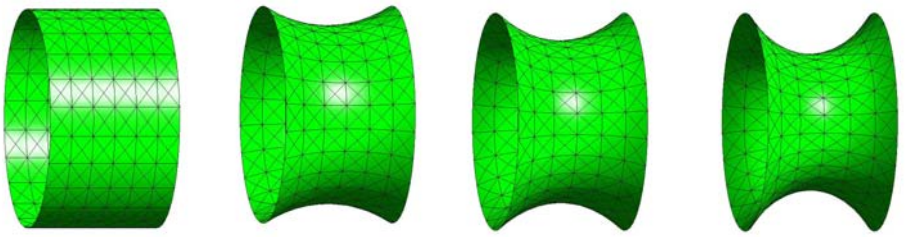

Figure 5. Deformation due to surface tension effect

In the limiting case this example amounts to that of finding the minimum surface of revolution. The analytical solution of this problem can be attained with recourse to variational calculus, for the given dimension, as $f(x)=1.8627\cosh(x/1.8627)$. The process of such deformation is depicted in the figure 5. Furthermore, figure 6 illustrates a comparison between the numerical and analytical result which proves the excellent efficiency of the proposed numerical scheme.

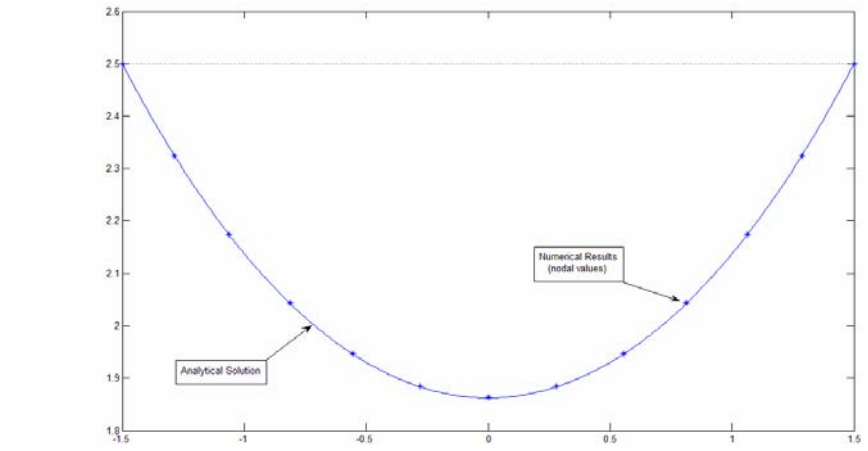

Figure 6. Numerical vs. Analytical solution

4. Conclusions

A finite element framework for continua with surface potentials has been presented. Based on geometry and kinematics of surfaces, the corresponding weak form of the balance equations accounting for contributions from the boundary is derived from the Dirichlet principle of minimum potential energy. A suitable framework for finite element implementation is given. Two models for boundary potentials are introduced and corresponding numerical examples have been provided, so as to confirm the efficiency of the proposed scheme. The solution procedure is robust and shows the asymptotically quadratic rate of convergence for Newton-Raphson scheme.

References

Adam NK (1941), *The physics and chemistry of surfaces*. London: Oxford University Press.

Adamson E, Gast AP (1997), *Physical chemistry of surfaces.* Wiley-Interscience.

Bellet M (2001), Implementation of surface tension with wall adhesion effects in a three-dimensional finite element model for fluid flow. *Communications in Numerical Methods in Engineering*, Volume 17, Issue 8:563 -- 579.

Ciarlet PG (2006), An Introduction to Differential Geometry with Applications to Elasticity. Springer.

Dettmer W, Peri c′ D (2006), A computational framework for free surface fluid flows accounting for surface tension. *Computer Methods in Applied Mechanics and Engineering*, Volume 195, Issues 23-24:3038--3071.

Dettmer W, Saksono PH, Peri c′ D (2003), On a finite element formulation for incompressible newtonian fluid flows on moving domains in the presence of surface tension. *Communications in Numerical Methods in Engineering*, Volume 19, Issue 9:659 -- 668.

Fischer FD, Waitz T, Vollath D, Simha NK (2008), On the role of surface energy and surface stress in phase-transforming nanoparticles. *Progress in Material Science*, 53:481--527.

Gibbs JW (1906), The scientific papers of J. Williard Gibbs. Vol. 1: Thermodynamics. New York and Bombay: Longmans, Green, and Co.

Gurtin ME (1975), A continuum theory for elastic material surfaces. *Archive for Rational Mechanics and Analysis*, 112:97--160.

Gurtin ME, Murdoch A (1975), A continuum theory of elastic material surfaces. *Archive of Rational Mechanics and Analysis*, 57, 291—323.

Javili A, Steinmann P (2009), A finite element framework for continua with boundary energies. Part I: The two-dimensional case. *Computer Methods in Applied Mechanics and Engineering*, 198, 27-29: 2198—2208.

Kuhl E, Askes H, Steinmann P (2004), An ale formulation based on spatial and material settings of continuum mechanics. part 1: Generic hyperelastic formulation. *Computer Methods in Applied* Mechanics *and Engineering*, 193:4207--4222.

Leo PH, Sekerka RF (1989), The effect of surface stress on crystal-melt and crystal-crystal equilibrium. *Acta metallurgica*, 37:3119--3138.

Lifshitz EM, Landau LD (1987), Fluid Mechanics, Second Edition: Volume 6 (Course of Theoretical Physics). Butterworth-Heinemann.

Marsden JE, Hughes TJR (1994), *Mathematical Foundations of Elasticity.* Dover Publications.

Navti SE, Ravindran K, Taylor C, Lewis RW (1997), Finite element modelling of surface tension effects using a lagrangian-eulerian kinematic description. *Computer Methods in Applied Mechanics and Engineering*, 147:41--60.

Olson L, Kock E (1994), A variational approach for modelling surface tension effects in inviscid fluids. *Computational Mechanics*, Volume 14, Number 2:140—153.

Saksono PH, Peric′ D (2006a), On finite element modelling of surface tension. Variational formulation and applications-Part I: Quasistatic problems. *Computational Mechanics*, Volume 38, 265--281.

Saksono PH, Peric′ D (2006b), On finite element modelling of surface tension. Variational formulation and applications-Part II: Dynamic problems. *Computational Mechanics*, Volume 38, 251--263.

Simha NK and Bhattacharya K (2000), Kinetics of phase boundaries with edges and junctions in a three-dimensional multiphase body. *Journal of Mech Phys Solids*, 48:2619--41.

Steinmann P, Häsner O (2005), On material interfaces in thermomechanical solids. *Archive of Applied Mechanics*, 75:31--41.

Steinmann P (2008), On boundary potential energies in deformational and configurational mechanics. *Journal of Mechanics and Physics of Solids*, 56, 3:772--800.

Zienkiewicz OC, Taylor RL (2005), The *Finite Element Method for Solid and Structural Mechanics*. Butterworth-Heinemann; 6 edition